Ultrafast dynamics and phonon softening in $Fe_{1+y}Se_{1-x}Te_x$ single crystals

2012 New J. Phys. 14 103053

(http://iopscience.iop.org/1367-2630/14/10/103053)

New Journal of Physics
The open-access journal for physics

Ultrafast dynamics and phonon softening in $Fe_{1+y}Se_{1-x}Te_x$ single crystals

C W Luo[1,7], I H Wu[1], P C Cheng[1], J-Y Lin[2], K H Wu[1], T M Uen[1], J Y Juang[1], T Kobayashi[1,3], Y C Wen[4], T W Huang[4], K W Yeh[4], M K Wu[4], D A Chareev[5], O S Volkova[6] and A N Vasiliev[6]

[1] Department of Electrophysics, National Chiao Tung University, Hsinchu 300, Taiwan
[2] Institute of Physics, National Chiao Tung University, Hsinchu 300, Taiwan
[3] Advanced Ultrafast Laser Research Center and Department of Engineering Science, Faculty of Informatics and Engineering, The University of Electro-Communications, 1-5-1 Chofugaoka, Chofu, Tokyo 182-8585, Japan
[4] Institute of Physics, Academia Sinica, Taipei 115, Taiwan
[5] Institute of Experimental Mineralogy, Chernogolovka, Moscow Region 142432, Russia
[6] Low Temperature Physics and Superconductivity Department, Moscow State University, 119991 Moscow, Russia
E-mail: cwluo@mail.nctu.edu.tw

New Journal of Physics **14** (2012) 103053 (13pp)
Received 10 April 2012
Published 31 October 2012
Online at http://www.njp.org/
doi:10.1088/1367-2630/14/10/103053

Abstract. The ultrafast quasiparticle dynamics of $Fe_{1+y}Se_{1-x}Te_x$ single crystals were investigated by dual-color transient reflectivity measurements ($\Delta R/R$) from 4.3 to 290 K. The electron–phonon coupling strength λ (= 0.16–0.01) and the temperature-dependent energy of longitudinal-acoustic phonons were, respectively, obtained from the relaxation time of a fast component and the period of an oscillation component in $\Delta R/R$. Such a small λ demonstrates the unconventional origin of superconductivity in FeSe. Moreover, the temperature-dependent $\Delta R/R$ exhibits anomalous changes at T_c, 90 K and 230 K, unambiguously revealing the phase transition as well as the phonon softening via the magnetoelastic effect.

[7] Author to whom any correspondence should be addressed.

Contents

1. Introduction

In 2008, the discovery of the superconductors $LaFeAsO_{1-x}F_x$ with a T_c around 26 K at ambient pressure [1] initiated investigations on the diversified family of Fe-based pnictides. Shortly afterwards, the T_c was further increased to 56 K by substituting La with other rare earths [2]. Since then, other Fe-based superconductors (FeSCs) have been successively found, including $Ba_{1-x}K_xAs_2Fe_2$ (122-type) with $T_c \leqslant 38$ K [3], LiFeAs (111-type) with $T_c \leqslant 18$ K [4] and FeSe (11-type) with $T_c \leqslant 10$ K [5]. In these new FeSCs, the interplay between electronic structure, phonons, magnetism and superconductivity is very rich and would help us understand the origin of high-T_c superconductivity. Among various FeSCs, however, the iron chalcogenide FeSe [5] stands out because of its structural simplicity, which consists of iron-chalcogenide layers stacking one another with the same Fe^{2+} charge state as the iron pnictides. Additionally, the T_c of FeSe has been increased further to 37 K at 7 GPa [6]; meanwhile, the partial replacement of Se with Te in FeSe also yields $T_c \sim 14$ K [7], which stimulated much interest in the properties of $FeSe_{1-x}Te_x$.

Recently, the existence of precursor superconductivity above T_c that competes with the spin-density wave order [8] and a pseudogap-like feature with onset around 200 K [9] were, respectively, observed on underdoped (Ba, K)Fe_2As_2 and nearly optimally doped $SmFeAsO_{0.8}F_{0.2}$ by optical pump–probe studies. Moreover, a coherent lattice oscillation was also found in Co-doped $BaFe_2As_2$ using time-resolved pump–probe reflectivity with 40 fs time resolution [10]. These results have unambiguously shown that femtosecond pump–probe spectroscopy is a protocol to study the simultaneous presence of electrons, phonons, magnons and the interactions between them. Therefore, further studies of the quasiparticle (QP) dynamics in FeSCs and its evolution with time and temperature are indispensable for understanding the mechanism of high-T_c superconductivity in FeSCs. In this paper, we report the time-resolved femtosecond spectroscopy study of the $Fe_{1+y}Se_{1-x}Te_x$ single crystals to elucidate the electronic structure and the QP dynamics.

2. Experiments

In this study, $Fe_{1.14}Te$ and $Fe_{1.05}Se_{0.2}Te_{0.8}$ single crystals were grown with an optical zone-melting technique [11]. The FeSe single crystals were grown in evacuated quartz ampoules using a $KCl/AlCl_3$ flux [12]. The crystalline structure of the samples was examined by

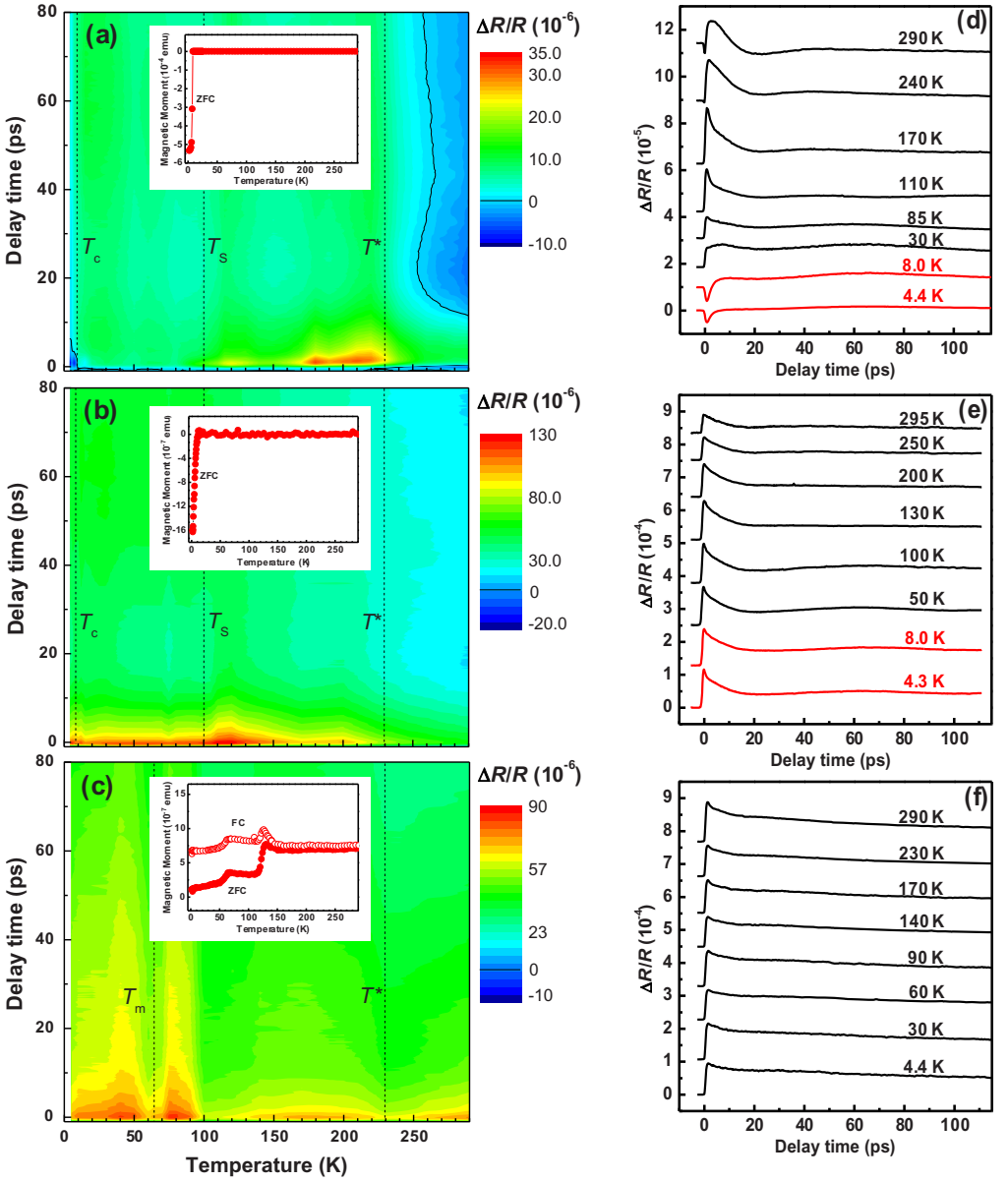

Figure 1. Temperature and delay time dependence of the two-dimensional (2D) $\Delta R/R$ in (a) FeSe, (b) $Fe_{1.05}Se_{0.2}Te_{0.8}$ and (c) $Fe_{1.14}Te$ single crystals. Insets show the temperature dependence of the magnetic susceptibility for (a) FeSe in $H = 20$ Oe, (b) $Fe_{1.05}Se_{0.2}Te_{0.8}$ in $H = 80$ Oe and (c) $Fe_{1.14}Te$ in $H = 80$ Oe. Panels (d)–(f) are the selected $\Delta R/R$ at some typical temperatures in panels (a), (b) and (c), respectively.

x-ray diffraction. The magnetic properties were obtained by temperature dependence of the magnetic susceptibility $\chi(T)$ as shown in the insets of figure 1. The superconducting transition temperatures of FeSe and $Fe_{1.05}Se_{0.2}Te_{0.8}$ are 8.8 and 10 K, respectively. For non-superconductive $Fe_{1.14}Te$, pronounced anomalies can be seen at 125 K in the inset of figure 1(c). Below this temperature, $\chi(T)$ exhibits clear irreversibility between zero-field cooling (ZFC)

and field cooling (FC) magnetization data. This may be due to the magnetite (Fe_3O_4) impurities and related to the Verwey transition, which is observed in magnetite at 120–125 K [13]. According to recent neutron-diffraction experiments in $Fe_{1+y}Te$ [14], the significant drop at 65 K (T_m) corresponds to an antiferromagnetic (AFM) ordering with a rather complex magnetic structure and to a simultaneous structural transition from tetragonal $P4/nmm$ symmetry to either monoclinic $P2_1/m$ or orthorhombic $Pmmn$ symmetry.

The femtosecond spectroscopy measurement was carried out using a dual-color pump–probe system (for the laser light source, the repetition rate is 5.2 MHz, the wavelength is 800 nm and the pulse duration is 100 fs) and an avalanche photodetector with the standard lock-in technique. The fluences of the pump beam and the probe beam are 2.48 and 0.35 $\mu J\,cm^{-2}$, respectively. The pump pulses have the corresponding photon energy (3.1 eV) where the higher absorption occurred in the absorption spectrum of FeSe [15] and hence can generate electronic excitations. The photo-induced QP dynamics is studied by measuring the photo-induced transient reflectivity changes ($\Delta R/R$) of a probe beam with a photon energy of 1.55 eV.

3. Temperature-dependent $\Delta R/R$

Figure 1 shows the 2D $\Delta R/R$ taken in $Fe_{1+y}Se_{1-x}Te_x$ single crystals. For the case of FeSe, there appear four temperature regions. Above 230 K, T^* (region I), there is a fast negative response with a relaxation time of about 1.5 ps together with a periodic oscillation in which the minima occur at ∼21 and ∼125 ps, respectively. When the temperature decreases below 230 K (region II), a positive and slow response appears and $\Delta R/R$ gradually becomes smaller until $T = 90$ K (T_s). Below 90 K (region III), the slow positive response disappears and is replaced by a complicated mixture of the positive and negative components as discussed later. For $T < T_c$ (region IV), a long-lived negative response appears like the one in region I. Qualitatively similar features were also observed in a $Fe_{1.05}Se_{0.2}Te_{0.8}$ single crystal as shown in figure 1(b). However, the negative oscillations above T^* were smeared due to the doping of Te and completely disappear on a fully Te-doped sample of $Fe_{1.14}Te$ as shown in figure 1(c). Additionally, in an $Fe_{1.05}Se_{0.2}Te_{0.8}$ single crystal (figure 1(b)) the positive $\Delta R/R$ becomes larger in amplitude with decreasing temperature. This temperature-dependent positive $\Delta R/R$ also markedly shows anomalies at 125 and 65 K in figure 1(c) of an $Fe_{1.14}Te$ single crystal, which are associated with the appearance of Fe_3O_4 impurities [13] and the magnetic phase transition [14, 16] as shown in the inset of figure 1(c), respectively.

In the pump–probe measurements, the electronic excitations generated by the pump pulses result in a swift rise of $\Delta R/R$ at zero time delay as shown in figure 2. The observed excitation was triggered by transferring the electrons from d valence band of Fe to d conduction band of Fe [17]. At zero time delay, the number of excited electrons generated by this non-thermal process is related to the amplitude of $\Delta R/R$. These high-energy electrons accumulated in the d conduction band of Fe release their energy through the emission of longitudinal-optical (LO) phonons within several picoseconds [18]. The LO phonons further decay into longitudinal-acoustic (LA) phonons via anharmonic interactions, i.e. transferring energy to the lattice. These relaxation processes can be detected using a probe beam as shown in figures 1 and 2. In the two-temperature model, the electrons and phonons (or lattice) are in thermal quasiequilibrium with two different time-dependent temperatures T_e and T_l. After the excitation of pump pulses, the increase of electron temperature is dramatically larger than that of phonons (T_e can reach several thousands of Kelvin above T_l) because of the much smaller heat capacity in the electron

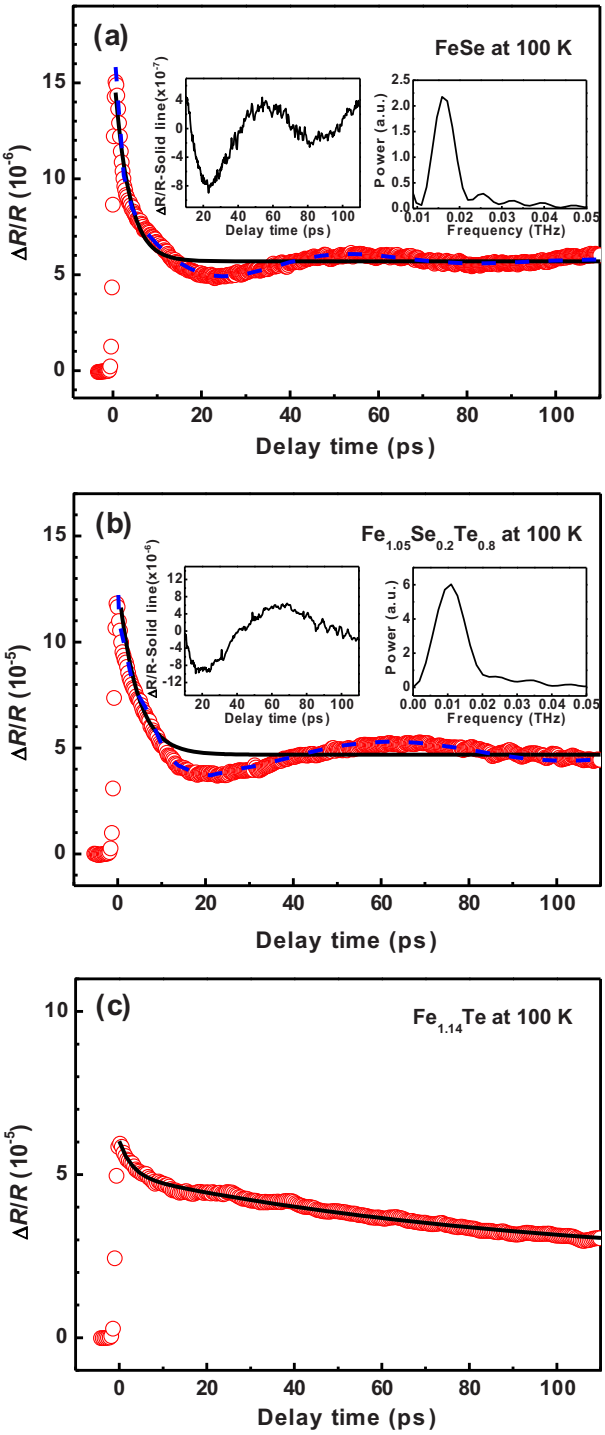

Figure 2. Selected $\Delta R/R$ curves for (a) FeSe, (b) $Fe_{1.05}Se_{0.2}Te_{0.8}$ and (c) $Fe_{1.14}Te$ single crystals. Dashed lines are the fitting curves using equation (1). Solid lines are the fitting curves without the oscillation component in equation (1). Insets show the oscillation component (subtract the solid line from the open circles) and their Fourier transformation.

subsystem. Then, both subsystem temperatures of electrons and phonons will become equal through electron–phonon coupling. Namely, the T_e decreases with a timescale of sub-ps to ps by transferring energy to phonons [19]. Following that, the T_l will decrease with a time scale of several ps to several hundreds of ps by phonon population decay (inelastic scattering) or dephasing (elastic scattering) [19]. According to the two-temperature model, relaxation processes ($t > 0$) of $\Delta R/R$ in $Fe_{1+y}Se_{1-x}Te_x$ single crystals can be phenomenologically described by

$$\frac{\Delta R}{R} = A_e\, e^{-t/\tau_e} + A_{LO}\, e^{-t/\tau_{LO}} + A_0 + A_{LA}\, e^{-t/\tau_{LA}} \sin\left(\frac{2\pi t}{T(t)} + \phi\right). \quad (1)$$

The first term in the right-hand side of equation (1) is the decay of A_e with a relaxation time τ_e, which is proportional to the initial excited electron (photoexcited QP) population number per unit cell [20]. In the second term, A_{LO} is proportional to the high-energy phonon population number per unit cell and decay with the relaxation time τ_{LO}. The third term describes energy loss from the hot spot to the ambient environment within the time scale of a microsecond, which is far longer than the period of the measurement ($\sim$150 ps) and hence is taken as a constant. The last term is the chirped oscillation component associated with strain pulse propagation[8]: A_{LA} is the amplitude of the oscillation; τ_{LA} is the damping time; $T(t)$ is the time-dependent period; and ϕ is the initial phase of the oscillation.

Like the dashed lines in figures 2(a) and (b), equation (1) can fit the $\Delta R/R$ data very well in FeSe and $Fe_{1.05}Se_{0.2}Te_{0.8}$ single crystals. However, the fitting for $\Delta R/R$ in $Fe_{1.14}Te$ has almost no need for the oscillation component in equation (1), as shown in figure 2(c). Consequently, each component in $\Delta R/R$ described above can be extracted using equation (1). The results of the extraction are shown in figure 3. For the negative and fast component (A_e) of $\Delta R/R$ only observed at $T > 230$ K and $T < 90$ K, it gradually increases as T decreases from 90 K; meanwhile, it also suppresses the positive and fast component that appeared at 100–200 K in figure 1(d). This trend is closely related to the strong AFM spin fluctuations below $T = T_s$ as revealed by ^{77}Se NMR measurements [23]. The relaxation of QP associated with the spin fluctuations between T_c and 90 K (in figure 3(b)) is $\sim$1.5–2 ps, which is almost temperature-independent. Intriguingly, as $T < T_c$, A_e dramatically shrinks as shown in the inset of figure 3(a); meanwhile, the QP relaxation time increases rapidly as shown in the inset of figure 3(b). Correspondingly, the spin–lattice relaxation rate $1/T_1$ also decreases rapidly due to the onset of superconductivity [23]. These certainly indicate that the growth of A_e associated with spin fluctuations at low temperatures is suppressed by the appearance of superconductivity. Thus, the spin fluctuations and superconductivity are competing factors in the FeSe system. The above results provide strong experimental evidence of competing orders in FeSe, which are consistent with the theoretical calculations [24]. It is noted that experimental evidence on

[8] In the displacive excitation of coherent phonon (DECP for absorbing media) mechanism [21], photoexcitation induces changes in the electronic energy distribution function, and consequently, the crystal lattice starts to oscillate around the new equilibrium position $A_0(t)$, which is proportional to the photoexcited carrier density $n(t)$. In the first order, only the A_{1g} totally symmetric modes are currently excited by the DECP mechanism. In 2002, Stevens *et al* [22] further solved the equation of motion for an LO vibrational mode to obtain the coherent phonon amplitude (or population), $A_{LO} \propto \mathrm{Im}(\varepsilon)$. Namely, the changes in phonon population A_{LO} cause a variation of the imaginary part of the dielectric constant ε. Then, changes in the imaginary part of ε vary the refractive index and cause further changes in reflectivity (R) in materials. Therefore, the $\Delta R/R$ in FeSe is proportional to the population of LO phonons, $\Delta R/R \propto A_{LO}$.

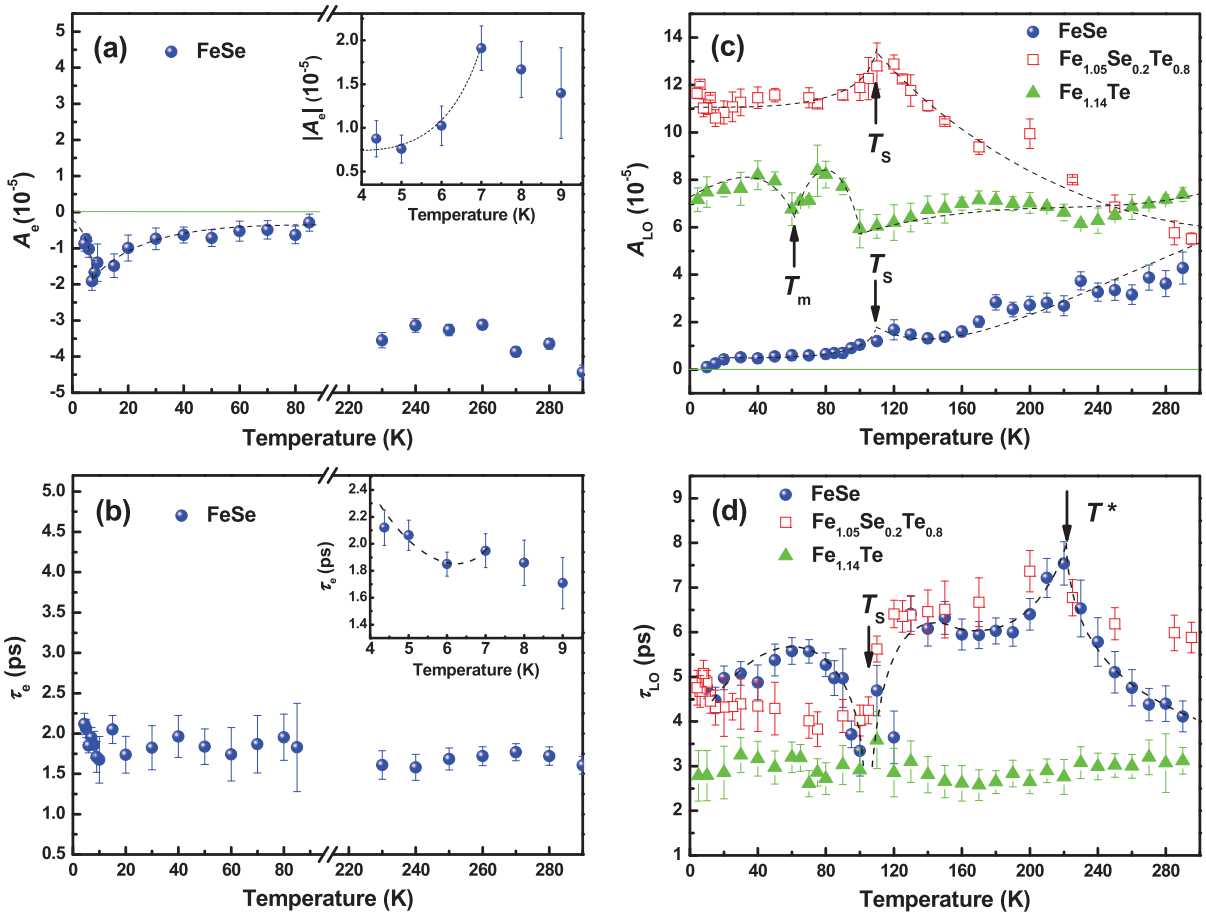

Figure 3. Temperature dependence of the amplitude (a) A_e, (c) A_{LO} and the relaxation time (b) τ_e, (d) τ_{LO} by fitting equation (1). Insets of (a) and (b) show a part of the temperature-dependent A_e and τ_{LO} on an enlarged scale. Dashed lines are a guide to the eyes.

the competing orders was also reported in the underdoped (Ba, K)Fe_2As_2 system [8]. The presence of a gap in the QP density of states gives rise to a bottleneck in carrier relaxation, which is clearly observed in the relaxation time τ_e close to T_c (see the inset of figure 3(b)). For the slower component (solid circles in figure 3(c)), the amplitude A_{LO} monotonically decreases as T decreases except for a small kink at T_s and then completely disappears in the superconducting state. In contrast, the relaxation time τ_{LO} (solid circles in figure 3(d)) exhibits two marked anomalies at both $T^* \sim 230$ K and $T_s \sim 90$ K. According to the scenario of relaxation processes described in [19] (see footnote 8), τ_{LO} is the relaxation time of LO phonon population via anharmonic decay into LA phonons. The divergences of temperature-dependent τ_{LO} at $T_s \sim 90$ K and $T^* \sim 230$ K imply a possibly efficient way or a bottleneck for the energy relaxation from LO phonons to LA phonons. If we take a look at the temperature-dependent LA phonon energy in figure 5, we only find one significant drop around 90 K, where the structural transition from the tetragonal phase to the orthorhombic phase occurs [25]. The smaller LA phonon energy causes the energy of LO phonons to more efficiently release to LA phonons and results in a significantly shorter relaxation time τ_{LO} around 90 K. Moreover, the structural

transition also leads to the more fluctuant τ_{LO} around 90 K. For an abnormally long relaxation time τ_{LO} of around 230 K, however, we cannot find any significant corresponding changes in the temperature-dependent LA phonon energy of figure 5. Thus, this bottleneck in the LO phonon energy transfer is possibly due to the photo-induced QPs rather than the LA phonons. As shown in figure 3(a), the sudden disappearance of A_e below 230 K may undermine the energy release efficiency of LO phonons. The sign change of the Seebeck coefficient of FeSe possibly due to an elusive higher-temperature phase transition was found to be also at T^* [26].

All the above anomalies of A_{LO} and τ_{LO} in FeSe were also found in superconductive $Fe_{1.05}Se_{0.2}Te_{0.8}$, but almost disappear in non-superconductive $Fe_{1.14}Te$. For the case of $Fe_{1.14}Te$, we only observed the abnormal changes of A_{LO} at $T_m \sim 65$ K and near 125 K, which were caused by the magnetic phase transition and the Verwey transition as shown in the inset of figure 1(c), respectively. This implies that the anomalies of A_{LO} and τ_{LO} at $T_s \sim 90$ K and $T^* \sim 230$ K may be associated with the superconductivity in FeSCs. Namely, both phase transition at $T^* \sim 230$ K and $T_s \sim 90$ K would be the key effect to cause superconductivity at low temperature [27].

4. Electron–optical phonon coupling strength

By fitting the $\Delta R/R$ curves with equation (1), dynamic information on QPs and phonons is available, which includes the number of QPs, the relaxation time of QPs and the energy of phonons. In a metal, the photo-induced QPs relaxation time is governed by transfer of energy from electrons to phonons with electron–phonon coupling strength λ [28]:

$$\frac{1}{\tau_e} = \frac{3\hbar\lambda\langle\omega^2\rangle}{\pi k_B T_e}, \tag{2}$$

where $\lambda\langle\omega^2\rangle$ is the second moment of the Eliashberg function and T_e can be further described by [29]

$$T_e = \left\langle \sqrt{T_i^2 + \frac{2(1-R)F}{l_s\gamma} e^{-z/l_s}} \right\rangle, \tag{3}$$

where T_i is the initial temperature of electrons, R is the unperturbed reflectivity at 400 nm, F is the pumping fluence and γ is the linear coefficient of heat capacity due to the electronic subsystem. The mean value is taken for the depth z going from the crystal surface down to the skin depth $l_s \sim 24$ nm (it was estimated from the skin depth of an electromagnetic wave in a metal, $\lambda/4\pi k$). All the parameters for the calculation of electron–phonon coupling strength are listed in table 1. For the estimation of $\langle\omega^2\rangle$, some vibrational modes are more efficiently coupled to QPs than others. In the case of Co-doped $BaFe_2As_2$, the symmetric A_{1g} mode is coherently excited by photoexcitation and efficiently coupled [10]. Consequently, we take the A_{1g} mode into account in the present case of $Fe_{1+y}Se_{1-x}Te_x$, which is the strongest phonon mode in the electron–phonon spectral function, $\alpha^2F(\omega)$ [17]. By equation (2), the consequent electron–phonon (A_{1g} mode) coupling strength, $\lambda = 0.16$, in FeSe. This value is consistent with the theoretical results of $\lambda = 0.17$ [17] obtained by using a linear response within the generalized gradient approximation. For the case of $Fe_{1.05}Se_{0.2}Te_{0.8}$, we obtained $\lambda = 0.01$, which is smaller than the value of $\lambda = 0.16$ in FeSe even if it possesses a higher $T_c \sim 10$ K. Furthermore, we can use the McMillan formula [34], $T_c = (\langle\omega\rangle/1.2)\exp\{-[1.40(1+\lambda)]/[\lambda - \mu^*(1+0.62\lambda)]\}$, to evaluate the critical temperature T_c. Taking $\langle\hbar\omega\rangle = 19.9$ meV and $\mu^* = 0$ [35], we obtain $T_c \sim 0.08$ K for FeSe and $\sim$0 K for $Fe_{1.05}Se_{0.2}Te_{0.8}$, which are far below the actual T_c of about

Table 1. The parameters for λ estimating at $T = 20$ K of the $Fe_{1+y}Se_{1-x}Te_x$ single crystals.

	T_c (K)	R (400 nm)	F (μJ cm^{-2})	γ[a] (mJ mol^{-1} K^{-2})	τ_e (ps)	A_{1g}[b] (meV)	$\lambda\langle\omega^2\rangle$[c] (meV^2)	λ
FeSe	8.8	0.25	9.92	5.73	1.75	19.9	61.3	0.16
$Fe_{1.05}Se_{0.2}Te_{0.8}$	10	0.20	15.76	57.5	4.32	20.0	4.5	0.01
$Fe_{1.14}Te$	–	0.11	17.36	32.0	2.86	19.7	4.0	0.01

[a]From [12, 30].
[b]From [31–33].
[c]Obtained from equation (2).

8.8 and 10 K, respectively. Therefore, the electron pairing mechanism in $Fe_{1+y}Se_{1-x}Te_x$ cannot be explained only by the electron–phonon interactions. Recently, the electron–phonon coupling strength of $\lambda \sim 0.12$ was measured in the $Ba(Fe_{0.92}Co_{0.08})_2As_2$ system, which is also too small to sustain its T_c of 24 K [36]. These results strongly imply that a phonon-mediated process cannot be the only mechanism leading to the formation of superconducting pairs in FeSCs.

5. Acoustic phonon softening

Further insight into the phase transition observed at ∼90 and ∼230 K in $Fe_{1+y}Se_{1-x}Te_x$ is provided by the study of the oscillation component of $\Delta R/R$. The temperature dependence of a strain pulse (LA phonons) propagation was clearly observed in the oscillation feature of $\Delta R/R$ after subtracting the decay background (i.e. the first, second and third terms in equation (1) and the solid lines in figure 2), as shown in figures 2(a) and (b) and 4. This oscillation is caused by the propagation of strain pulses inside $Fe_{1+y}Se_{1-x}Te_x$ single crystals, namely the interference between the probe beams reflected from the crystal surface and the wave front of the propagating strain pulse [37]. At high temperatures, the damping time is very short and the oscillation is sustained only for one period. However, the number of oscillation periods markedly increases around 100 K in FeSe (see figure 4(a)); hence, the damping time becomes much longer. Besides, the oscillation period significantly increases below 90 K. This means that the LA phonons can propagate further into the interior of FeSe crystals with orthorhombic structure. Similar features were also observed in $Fe_{1.05}Se_{0.2}Te_{0.8}$. Nevertheless, the characteristics of the temperature-dependent oscillation component in superconductive FeSe and $Fe_{1.05}Se_{0.2}Te_{0.8}$ are almost obscured in the non-superconductive $Fe_{1.14}Te$.

By Fourier transformation of the oscillation component at $T = 100$ K in the right inset of figure 2(a) of FeSe, the phonon frequency is found to be 16 GHz. The phonon energy is estimated to be ∼0.07 meV. The coherent acoustic phonon detected by a pump–probe reflectivity measurement can be described as a Brillouin scattering [38] phenomenon occurring in the materials after excitation of pump pulses. The scattering condition is $q_{phonon} = 2nk_{probe}\cos(\theta_i)$, where q_{phonon} is the phonon wave vector, n is the real part of the refractive index, and the probe photon has a wave vector k_{probe} arriving at an incident angle θ_i (inside crystals) with respect to the surface normal. Following this scattering condition, the probe beam acts as a filter to select the acoustic wave propagating along the scattering plane symmetry axis, i.e.

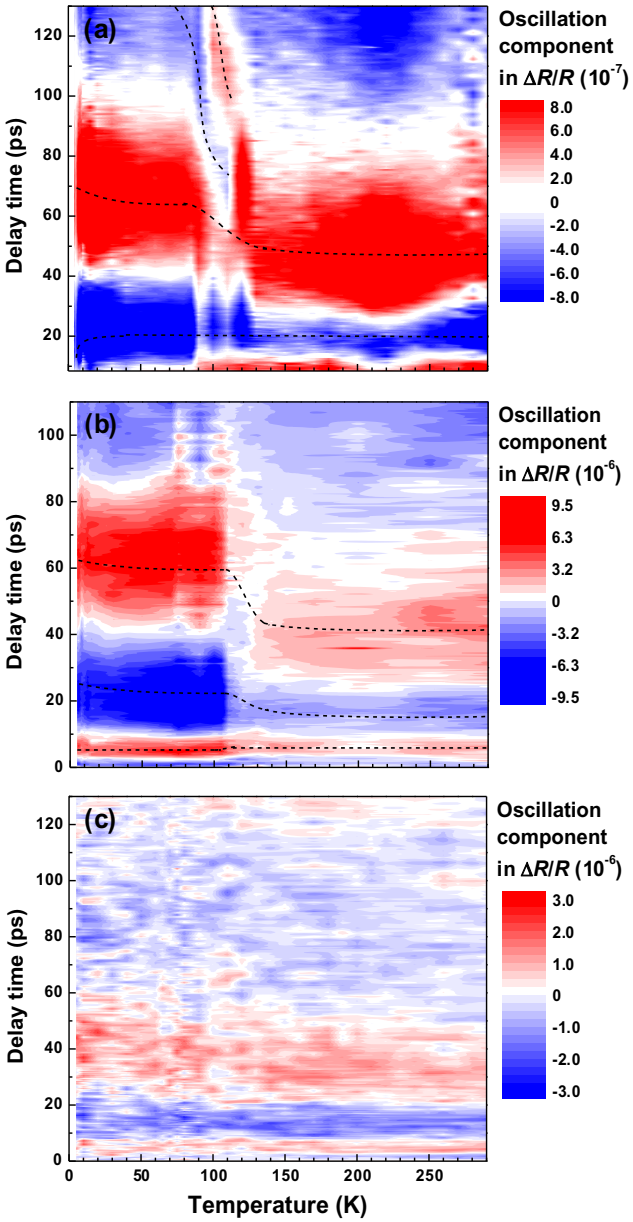

Figure 4. Temperature-dependent oscillation component of $\Delta R/R$ in (a) FeSe, (b) $Fe_{1.05}Se_{0.2}Te_{0.8}$ and (c) $Fe_{1.14}Te$ single crystals, which were obtained by subtracting the decay background (the first, second and third terms in equation (1)) from $\Delta R/R$ of figure 1. Dashed lines are a guide to the eyes.

the normal to the crystal surface, and traveling with the wave vector q_{phonon}. The energy of the acoustic wave is

$$E_{\text{phonon}} = \hbar\omega_{\text{phonon}} = \hbar q_{\text{phonon}} v_{\text{s}} = \hbar 2 n v_{\text{s}} k_{\text{probe}} \cos(\theta_{\text{i}}), \tag{4}$$

where v_{s} is the sound velocity along the normal direction of the crystal surface. Using $\lambda_{\text{probe}} = 800\,\text{nm}$, $n_{\text{probe}} = 2$ [15], $\theta_{\text{i}} = 2.5^{\circ}$ (estimated from the incident angle (5°) of the probe beam by Snell's law) and $v_{\text{s}} = 3.58\,\text{km}\,\text{s}^{-1}$ [39], the phonon energy, E_{phonon}, is calculated to be

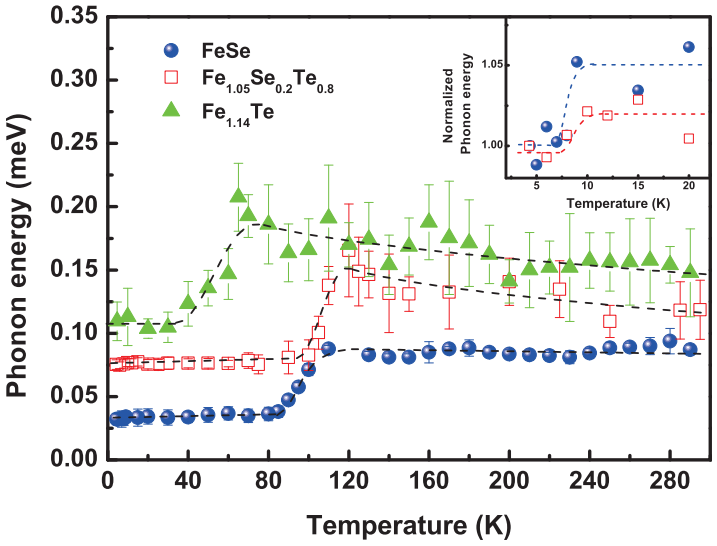

Figure 5. Temperature dependence of the phonon energy derived from the oscillation component in figure 4. The inset shows a part of the temperature-dependent phonon energy on an enlarged scale. Dashed lines are a guide to the eyes.

0.077 meV, which is very close to the result, 0.07 meV, directly obtained from the above $\Delta R/R$ measurements.

Moreover, we further investigate the temperature dependence of the LA phonon energy as shown in figure 5. For the case of FeSe, the phonon energy dramatically drops by 60%[9] around 90 K where a structural phase transition occurs, and then remains constant at low temperatures. Additionally, we found that the LA phonons also soften by 6% in the superconducting state as shown in the inset of figure 5, which is consistent with the larger distance between the first depth and the first peak in figure 4(a). Very recently, the phonon softening near the structure transition in $BaFe_2As_2$ and Co-doped $BaFe_2As_2$ was observed by inelastic x-ray scattering [40] and resonant ultrasound spectroscopy [27, 41], respectively. Fernandes *et al* [27] found 16% softening of shear modulus in $BaFe_{1.84}Co_{0.16}As_2$ at $T_c = 22$ K. For the non-superconducting case of $BaFe_2As_2$, however, a rather large softening of 90% was observed around 130 K, where the structural and AFM phase transition temperature occurs. Similarly, a large phonon softening due to structural phase transition and a rather small phonon softening due to the superconducting phase transition were also unambiguously observed in superconductive FeSe and $Fe_{1.05}Se_{0.2}Te_{0.8}$. These results suggest that the reduction of phonon energy at both the structural and the superconducting phase transition is a general feature of FeSCs. The above phonon softening may participate in superconductive pairing, albeit not the mechanism responsible for high T_c in FeSCs. Additionally, in the non-superconductive $Fe_{1.14}Te$ a marked anomaly was clearly observed at around 65 K, which is just the temperature of magnetic phase transition as shown in the inset of figure 1(c). Namely, the LA phonons in $Fe_{1.14}Te$ softened with the appearance of AFM ordering through the magnetoelastic effect. In Kulić and Haghighirad's theoretical calculations [42], they also predicted the existence of giant magnetoelastic effects at

[9] Assume that the refractive index n of FeSe is temperature-independent.

the transition from the magnetic state to the non-magnetic state in Fe-pnictides. Consequently, the phonon softening in FeSe and $Fe_{1.05}Se_{0.2}Te_{0.8}$ accompanying the simultaneous appearance of spin fluctuations shown in figure 3(a) may also be caused by the magnetoelastic effect.

6. Summary

We have studied the ultrafast QP dynamics and phonon softening in $Fe_{1+y}Se_{1-x}Te_x$ single crystals by dual-color femtosecond spectroscopy. From the relaxation time τ_e of $\Delta R/R$, the electron–phonon coupling strength was obtained to be $\lambda = 0.16$ for FeSe and $\lambda = 0.01$ for $Fe_{1.05}Se_{0.2}Te_{0.8}$. The anomalous changes of amplitude (A_e, A_{LO}) and relaxation time (τ_e, τ_{LO}) in the temperature-dependent $\Delta R/R$ are clearly observed at 90 K (T_s) and 230 K (T^*) and show the existence of phase transition in FeSe and $Fe_{1.05}Se_{0.2}Te_{0.8}$. Moreover, the energy of LA phonons as a function of temperature estimated from the oscillation component of $\Delta R/R$ markedly softens at T_c and the temperatures of the structural and magnetic phase transitions through the magnetoelastic effects. Our results provide a vital understanding of the competing picture between the spin fluctuations and the superconductivity, and the role of phonons in Fe-based superconductors.

Acknowledgments

This project was financially sponsored by the National Science Council (grant no. NSC 98-2112-M-009-008-MY3) and the Ministry of Education (the MOE-ATU plan at National Chiao Tung University). The support from Russian Ministry of Science and Education through Grants 11.519.11.6012, 14.740.11.1365 and Russian Foundation for Basic Research through Grants 10-02-00021, 12-02-90405 and 12-02-90823 is acknowledged. DAC acknowledges support through Grant of President of Russian Federation for State Support of Young Russian Scientists (MK-1557.2011.5) and Russian Ministry of Education and Science through Grant N83-78.

References

[1] Kamihara Y, Watanabe T, Hirano M and Hosono H 2008 *J. Am. Chem. Soc.* **130** 3296–7
[2] Wang C *et al* 2008 *Europhys. Lett.* **83** 67006
[3] Rotter M, Tegel M and Johrendt D 2008 *Phys. Rev. Lett.* **101** 107006
[4] Wang X C, Liu Q Q, Lv Y X, Gao W B, Yang L X, Yu R C, Li F Y and Jin C Q 2008 *Solid State Commun.* **148** 538
[5] Hsu F C *et al* 2008 *Proc. Natl Acad. Sci. USA* **105** 14262
[6] Margadonna S, Takabayashi Y, Ohishi Y, Mizuguchi Y, Takano Y, Kagayama T, Nakagawa T, Takata M and Prassides K 2009 *Phys. Rev.* B **80** 064506
[7] Sales B C, Sefat A S, McGuire M A, Jin R Y and Mandrus D 2009 *Phys. Rev.* B **79** 094521
[8] Chia E E M *et al* 2010 *Phys. Rev. Lett.* **104** 027003
[9] Mertelj T, Kabanov V V, Gadermaier C, Zhigadlo N D, Katrych S, Karpinski J and Mihailovic D 2009 *Phys. Rev. Lett.* **102** 117002
[10] Mansart B, Boschetto D, Savoia A, Rullier-Albenque F, Forget A, Colson D, Rousse A and Marsi M 2009 *Phys. Rev.* B **80** 172504
[11] Yeh K W, Ke C T, Huang T W, Chen T K, Huang Y L, Wu P M and Wu M K 2009 *Cryst. Growth Des.* **9** 4847
[12] Luo C W *et al* 2012 *Phys. Rev. Lett.* **108** 257006
[13] Walz F 2002 *J. Phys.: Condens. Matter* **14** R285

[14] Rodriguez E E, Stock C, Zajdel P, Krycka K L, Majkrzak C F, Zavalij P and Green M A 2011 *Phys. Rev.* B **84** 064403
[15] Wu X J *et al* 2007 *Appl. Phys. Lett.* **90** 112105
[16] Gnezdilov V *et al* 2011 *Phys. Rev.* B **83** 245127
[17] Subedi A, Zhang L, Singh D J and Du M H 2008 *Phys. Rev.* B **78** 134514
[18] Krasniqi F S, Johnson S L, Beaud P, Kaiser M, Grolimund D and Ingold G 2008 *Phys. Rev.* B **78** 174302
[19] Hase M, Ishioka K, Demsar J, Ushida K and Kitajima M 2005 *Phys. Rev.* B **71** 184301
[20] Kabanov V V, Demsar J, Podobnik B and Mihailovic D 1999 *Phys. Rev.* B **59** 1497
[21] Zeiger H J, Vidal J, Cheng T K, Ippen E P, Dresselhaus G and Dresselhaus M S 1992 *Phys. Rev.* B **45** 768
[22] Stevens T E, Kuhl J and Merlin R 2002 *Phys. Rev.* B **65** 144304
[23] Imai T, Ahilan K, Ning F L, McQueen T M and Cava R J 2009 *Phys. Rev. Lett.* **102** 177005
[24] Shi H, Huang Z B, Tse J S and Lin H Q 2011 *J. Appl. Phys.* **110** 043917
[25] McQueen T M, Williams A J, Stephens P W, Tao J, Zhu Y, Ksenofontov V, Casper F, Felser C and Cava R J 2009 *Phys. Rev. Lett.* **103** 057002
[26] McQueen T M *et al* 2009 *Phys. Rev.* B **79** 014522
[27] Fernandes R M, VanBebber L H, Bhattacharya S, Chandra P, Keppens V, Mandrus D, McGuire M A, Sales B C, Sefat A S and Schmalian J 2010 *Phys. Rev. Lett.* **105** 157003
[28] Allen P B 1987 *Phys. Rev. Lett.* **59** 1460
[29] Boschetto D, Gamaly E G, Rode A V, Luther-Davies B, Glijer D, Garl T, Albert O, Rousse A and Etchepare J 2008 *Phys. Rev. Lett.* **100** 027404
[30] Liu T J *et al* 2010 *Nature Mater.* **9** 718
[31] Kumar P, Kumar A, Saha S, Muthu D V S, Prakash J, Patnaik S, Waghmare U V, Ganguli A K and Sood A K 2010 *Solid State Commun.* **150** 557
[32] Okazaki K, Sugai S, Niitaka S and Takagi H 2011 *Phys. Rev.* B **83** 035103
[33] Xia T-L, Hou D, Zhao S C, Zhang A M, Chen G F, Luo J L, Wang N L, Wei J H, Lu Z-Y and Zhang Q M 2009 *Phys. Rev.* B **79** 140510
[34] McMillan W L 1968 *Phys. Rev.* **167** 331
[35] Boeri L, Dolgov O V and Golubov A A 2008 *Phys. Rev. Lett.* **101** 026403
[36] Mansart B, Boschetto D, Savoia A, Rullier-Albenque F, Bouquet F, Papalazarou E, Forget A, Colson D, Rousse A and Marsi M 2010 *Phys. Rev.* B **82** 024513
[37] Thomsen C, Grahn H T, Maris H J and Tauc J 1986 *Phys. Rev.* B **34** 4129
[38] Brillouin L 1922 *Ann. Phys.* **17** 88
[39] Chandra S and Islam A K M A 2010 *Physica* C **470** 2072
[40] Niedziela J L, Parshall D, Lokshin K A, Sefat A S, Alatas A and Egami T 2011 *Phys. Rev.* B **84** 224305
[41] Goto T, Kurihara R, Araki K, Mitsumoto K, Akatsu M, Nemoto Y, Tatematsu S and Sato M 2011 *J. Phys. Soc. Japan* **80** 073702
[42] Kulić M L and Haghighirad A A 2009 *Europhys. Lett.* **87** 17007